IJAMML 2:1 (2015) 9-26 March 2015
ISSN: 2394-2258
Available at http://scientificadvances.co.in

MEDICAL IMAGE FUSION BASED ON QUATERNION WAVELET TRANSFORM AND VISIBILITY FEATURE

Peng Geng[a], Xing Su[a] and Tan Xu[b]

[a]School of Information Science and Technology, Shijiazhuang Tiedao University, Shijiazhuang, P. R. China

[b]School of Physics, Hengshui University, Hengshui, P. R. China

Abstract

Medical image fusion is the process of registering and combining multiple images from single or multiple imaging modalities to improve the imaging quality and reduce redundant information. In this research, a fusion algorithm is proposed to combine one pairs of medical images, such as the CT-MRI images and CT-MRA images. The source medical images are firstly decomposed by the quaternion wavelet transform. In this method, the visibility feature conformed to human visual system is adopted to fused the quaternion wavelet coefficients. Owing to the shift-invariance of the quaternion wavelet coefficients, the proposed method is effective and can get satisfactory fusion results. This new method provides improved subjective and objectives results as compared to previous image fusion methods based on the redundant discrete wavelet transform, nonsubsampled contourlet transform, ripplet transform, and the NSDFB-DTCWT transform.

Keywords: QWT, image fusion, visibility feature.

*Corresponding author.
E-mail address: gengpeng@stdu.edu.cn (Peng Geng).

2010 Mathematics Subject Classification: 68.
Submitted by Shuaiqi Liu.
Received January 25, 2015; Revised March 11, 2015

1. Introduction

With the development of medical science, the computer science and biological engineering technology, various modalities of medical images have become available, such as X-ray, computed tomography (CT), magnetic resonance imaging (MRI), magnetic resonance angiography (MRA), and positron emission tomography (PET) images [1]. These multimodal medical images usually provide complementary and occasionally conflicting information. Image fusion can be broadly defined as the process of combining multiple input images or some of their features into a single image without the introduction of distortion or loss of information. Since computer aided imaging techniques enable a quantitative assessment of the images under evaluation, it helps to improve the efficacy of the medical practitioners in arriving at an unbiased and objective decision in a short span of time. Image fusion algorithms can be classified as four levels of abstraction: signal level, pixel level, feature level, and symbolic level. At the pixel-level method, images are combined by considering individual pixel values or small arbitrary regions of pixels in order to make the fusion decision. This paper focuses on the pixel-level medical image fusion.

Recently, a lot of medical image fusion methods have been emerged, such as intensity-hue-saturation (IHS), principal component analysis (PCA), Brovey transform and multiscale geometry analysis (MGA). Specially, the fusion approaches adopting the based-MGA method can be classified as wavelet transform, contourlet transform, nonsubsampled contourlet transform (NSCT), and ripplet transform etc. [2]. Singh proposed a medical image fusion algorithm based on redundant discrete wavelet transform in [3] and the paper in [4] also gave a medical image fusion algorithm by using contourlet. Combined with nonsubsampled direction filter bank-dual-tree complex wavelet transform (NSDFB-DTCWT) [5], a medical image fusion algorithm based on NSDFB-DTCWT is proposed to overcome the complexity fusion rules in image fusion

algorithm based on the multi-scale multi-resolution transform. A multimodality medical image fusion method, based on ripplet is presented by Sudeb [6]. An efficient image fusion approach which applies fusion rules to the nonsubsampled contourlet transform decomposition coefficients of the transmission image and the reflection image for ultrasound tomography is proposed [7]. The shift-invariant shearlet transform is used to the multimodal medical image fusion in [8]. The region sum-weighted and local energy fusion rule is separately used in the lowpass subband and highpass subbands. Although some good results had been achieved based on the image fusion algorithms above, but it can be concluded that efforts should be made to improve the objective and subjective effect of these methods.

The NSCT, as a fully shift-invariant form of contourlet leads to better frequency selectivity and regularity. Shearlet transform forms a tight frame at various scales and directions, and is optimally sparse in representing images with edges. But there are more redundant in the NSCT decomposition and shearlet decompositions, so the fusion methods based on NSCT or shearlet are slower than other multiscale decomposition methods [7, 8]. The contourlet transform offers flexible multi-resolution and multi-directional decomposition for images. The major problem with the DWT comes from its shift variant characteristic caused by subsampling operation. A shift-invariant DWT (SIDWT), described in [9], yields a very over-complete signal representation as there is no subsampling. However, any CWT based on wavelets of compact support cannot exactly possess the Hilbert transform, and this means that any such CWT will not perfectly overcome the disadvantage of the traditional DWT [10]. The quaternion wavelet transforms (QWT) [11] proposed by Corrochano is a new multiscale analysis theory to capture the geometry features of an image. The QWT coefficients have three phases content beside the magnitude information. The QWT is a near shift-invariant [12]. In this paper, a new medical image fusion method has been proposed based on the quaternion wavelet transform.

2. Quaternion Wavelet Transform

QWT is the extension of complex wavelet transform that provides the richer scale-space represent for 2-D signals geometric structure. The QWT can provide more coefficients in the decomposing the images than the DWT, DTCWT, and SIDWT. Secondly, in practice, the image fusion method performance quickly deteriorates when there is slight object movement or when the source multi-modal images cannot be perfectly registered. Hence, the QWT method can overpass the DWT method and DT-CWT method in the multi-modal medical images fusion. Except for the near shift-invariant, the QWT inherits many of other interesting and useful theoretical properties, such as the quaternion phase representation and symmetry properties. Contrary to the DWT, it is near shift-invariant and provides a magnitude-phases local analysis of images [13, 14]. Furthermore, the QWT can be computed by using a 2-D dual-tree filter bank with linear computational complexity. For convenience of further discussions, we briefly review some basic ideas about the quaternion algebra and the construction of QWT.

The quaternion algebra over R, denoted by H, is an associative non-commutative four-dimensional algebra:

$$H = \{q = a + bi + cj + dk \,|\, a, b, c, d \in R\}, \tag{1}$$

which obeys Hamilton's multiplication rules.

$$ij = -ji = k,\ jk = -kj = i,\ ki = -ik = j,\ i^2 = j^2 = k^2 = ijk = -1. \tag{2}$$

An alternative representation for a quaternion is

$$q = |q| e^{i\varphi} e^{k\psi} e^{j\theta}, \tag{3}$$

where $(\varphi, \psi, \theta) \in [-\pi, \pi) \times [-\pi/2, \pi/2) \times [-\pi/4, \pi/4)$. It is defined by one modulus and three angles that we call phase. When $\psi \in [-\pi/4, \pi/4)$, the computational formula is

$$\begin{cases} \varphi = \arctan\left(\dfrac{2(ac+bd)}{a^2+b^2-c^2-d^2}\right), \\ \theta = \arctan\left(\dfrac{2(ab+cd)}{a^2+b^2-c^2-d^2}\right), \\ \psi = -\dfrac{1}{2}\arcsin(2ad-2bd). \end{cases} \tag{4}$$

The quaternion analytic signal is defined by its partial $(H_1,\ H_2)$ and total (H_T) Hilbert transforms (HT).

$$f_A(x,\ y) = f(x,\ y) + iH_1(f(x,\ y)) + jH_2(f(x,\ y)) + kH_T(f(x,\ y)), \tag{5}$$

where $H_1(f(x,\ y)) = f(x,\ y)^{**}(\delta(y)/\pi x)$, $H_2(f(x,\ y)) = f(x,\ y)^{**}(\delta(x)/\pi y)$, and $H_{T1}(f(x,\ y)) = f(x,\ y)^{**}\left(1/\pi^2 xy\right)$. $\delta(y)$ and $\delta(x)$ are impulse sheets along x and y axes, respectively. And ** denotes 2-D convolution.

We start with real separable scaling function φ and mother wavelets $\psi^H,\ \psi^V,\ \psi^D,$ for separable wavelet, $\psi(x,\ y) = \psi_h(x)\psi_h(y)$. According to the definition of the quaternary analytic signal, the analytic 2-D wavelets can be constructed as follows:

$$\begin{cases} \varphi = \varphi_h(x)\varphi_h(x) \to \varphi + iH_1(\varphi) + jH_2(\varphi) + kH_T(\varphi), \\ \psi^H = \psi_h(x)\varphi_h(y) \to \psi^H + iH_1(\psi^\nu) + jH_2(\psi^\nu) + kH_T(\psi^\nu), \\ \psi^\nu = \varphi_h(x)\psi_h(y) \to \psi^\nu + iH_1(\psi^\nu) + jH_2(\psi^\nu) + kH_T(\psi^\nu), \\ \psi^D = \psi_h(x)\psi_h(y) \to \psi^D + iH_1(\psi^D) + jH_2(\psi^D) + kH_T(\psi^D). \end{cases} \tag{6}$$

For separable wavelet, $\psi(x,\ y) = \psi_h(x)\psi_h(y)$ 2-D HT equals to twice 1-D HT along row and column, respectively. Considering that 1-D HT pair, i.e., $\psi_h,\ \psi_g = H\psi_h$ and scaling function $\varphi_h,\ \varphi_g = H\varphi_h,$ 2-D analytic wavelet can be derived from formula (6) as the product form of 1-D separate wavelet.

$$\begin{cases} \varphi = \varphi_h(x)\varphi_h(y) + i\varphi_g(x)\varphi_h(y) + j\varphi_h(x)\varphi_g(y) + k\varphi_g(x)\varphi_g(y), \\ \psi^H = \psi_h(x)\varphi_h(y) + i\psi_g(x)\varphi_h(y) + j\psi_h(x)\varphi_g(y) + k\psi_g(x)\varphi_g(y), \\ \psi^V = \psi_h(x)\psi_h(y) + i\varphi_g(x)\psi_h(y) + j\varphi_h(x)\psi_g(y) + k\psi_g(x)\varphi_g(y), \\ \psi^D = \psi_h(x)\psi_h(y) + i\psi_g(x)\varphi_h(y) + j\psi_h(x)\psi_g(y) + k\psi_g(x)\varphi_g(y). \end{cases} \tag{7}$$

The real-imaginary quaternion analytic form can be transformed into magnitude-phase form as (3) according to (4). The QWT magnitude $|q|$, with the property of near shift-invariance, represents features at any spatial position in each frequency sub-band, and the three phases (φ, ψ, θ) describe the 'structure' of those features. More details about implementation of QWT used here are referenced to the work [11, 12, 13].

3. Fusion Rule

This approach is motivated by the fact that the human visual system is sensitive to the contrast. Hence, the visibility of image [15] can be likely to provide better details and conform to the human observer. Adopting the visibility feature of the image, the fusion rule firstly calculates the window-based local mean of the quaternion wavelet coefficient. Local mean of quaternion wavelet coefficient in the window W can be expressed as

$$LM^l(i, j) = \frac{1}{MN} \sum_{m,n \in W} Q^l(i + m, j + n), \tag{8}$$

where $Q^l(i, j)$ is the value of quaternion wavelet coefficients at scale l. The M and N decide the width and height of the window W. Therefore, the visibility feature of quaternion wavelet coefficients should be calculated as

$$V^l(i, j) = \frac{1}{LM^l(i, j)^\alpha} \left(LM^l(i, j) \times Q^l(i, j) - LM^l(i, j) \right). \tag{9}$$

After calculating the visibility feature of all quaternion wavelet coefficients including the high frequency subband and the low frequency subband, the decision map can be calculated.

$$map^{l}(i,\ j) = \begin{cases} 1, & \text{if } V_A^l(i,\ j) >= V_B^l(i,\ j), \\ 0, & \text{if } V_B^l(i,\ j) < V_A^l(i,\ j), \end{cases} \tag{10}$$

where $V_A^l(i,\ j)$ and $V_B^l(i,\ j)$ is the local mean according to Equation (9) by the quaternion wavelet coefficients of source image A and B. The corresponding coefficients with higher magnitude of visibility are then chosen into the fused image as follows:

$$Q_F^l(i,\ j) = \begin{cases} Q_A^l(i,\ j), & \text{if } map^{l}(i,\ j) = 1, \\ Q_B^l(i,\ j), & \text{if } map^{l}(i,\ j) = 0, \end{cases} \tag{11}$$

where $Q_F^l(i,\ j)$, $Q_A^l(i,\ j)$, and $Q_B^l(i,\ j)$ are the coefficient of the fused images F, source image A, and source image B located at the i-th row and j-th column in the l-th scale, respectively.

4. Proposed Fusion Approach

Figure 1 shows the block diagram of the proposed method, which consists of a number of essential stages:

Step 1. The multimodal medical images to be fused are registered to assure that the corresponding pixels are aligned.

Step 2. The source images are decomposed into different directions and scales using the QWT.

Step 3. Quaternion wavelet coefficients of the final fused image are obtained via visibility feature of quaternion wavelet coefficients obtained using Equation (11).

Step 4. The inverse QWT of the new fused low and high frequency coefficients is performed to generate the final fused image.

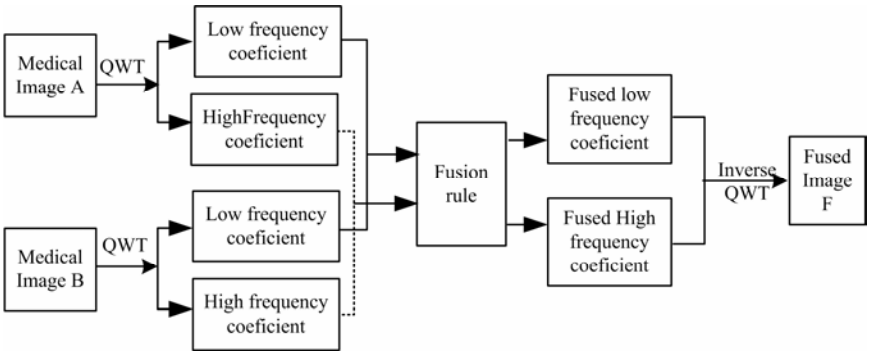

Figure 1. Schematic diagram of fusion algorithm based on QWT.

5. Experiments

For verifying the effectiveness of the proposed method, four pairs of medical images are adopted to experiment. The four pairs of images can be separated into four groups shown in Figure 2. The group a, b, and c are CT-MRI images, respectively. The group d is MRA-MRI images, respectively. The performance of the proposed method is compared with the redundant discrete wavelet transform (RDWT) method proposed by Richa [3], the spatial frequency of NSCT coefficients motivated PCNN method [16] proposed by Qu, the modified spatial frequency of ripplet coefficients motivated PCNN method proposed by Sudeb [6], and the dual-tree complex wavelet transform method combined with the nonsubsampled direction filter bank (NSDFB) by Liu [5]. In the Qu's method, the pyramid filter and the direction filter are set to 'pyrexc' and 'vk', respectively. The decomposition levels are set to [0, 1, 3, 3, 4]. In the Sudeb's ripplet method, the parameters of the '9/7' filter, 'pkva' filter and levels = [0, 1, 2, 3] are used to decompose the source images by ripplet transom. In the Richa's RDWT method, the source images are decomposed by two levels of 'db6' wavelet filters. The three levels of dual-tree complex wavelet transform are adopted to decompose the NSDFB coefficients in the Liu's method. The direction filter is set to 'cd'. In the proposed method, the one level of quaternion wavelet decomposition is adopted.

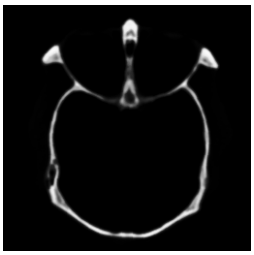

(a) CT

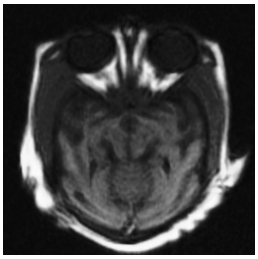

(b) MRI

Group a

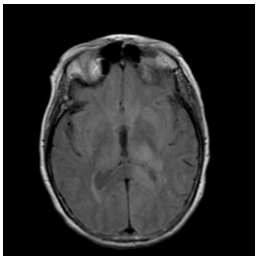

(c) CT

(d) MRI

Group b

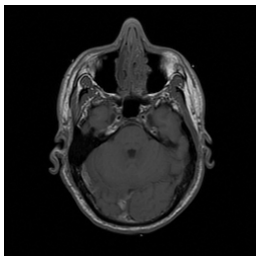

(e) CT

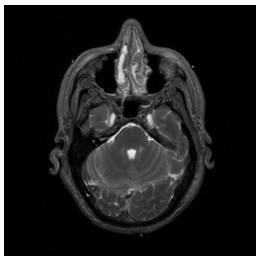

(f) MRA

Group c

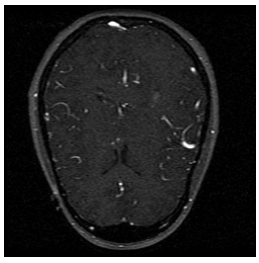

(g) MRA

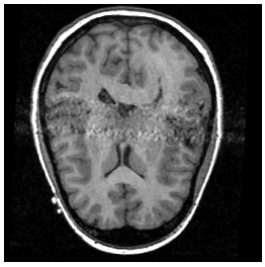

(h) T1-MRI

Group d

Figure 2. Test images.

Two metrics are considered in this paper, which do not require ground truth images for evaluation. The first metric is $Q^{AB/F}$ [16], which considers the amount of edge information transferred from the input images to the fused image using a Sobel edge detector to calculate the strength and orientation information at each pixel in both source and the fused images. The second metric is the mutual information (MI) metric [17] used to evaluate the fusion performance quantitatively in this paper. Table 1 shows the performance results from different image fusion methods and different datasets. The results presented in this example can demonstrate that our approach can fuse the medical images while retains much more information than that of the other two methods.

The visual comparison for fused images according to different fusion algorithms are shown in Figures 3, 4, 5, and 6, respectively. From the four figures, it is clear that the proposed algorithm improves better detail information than the other algorithms.

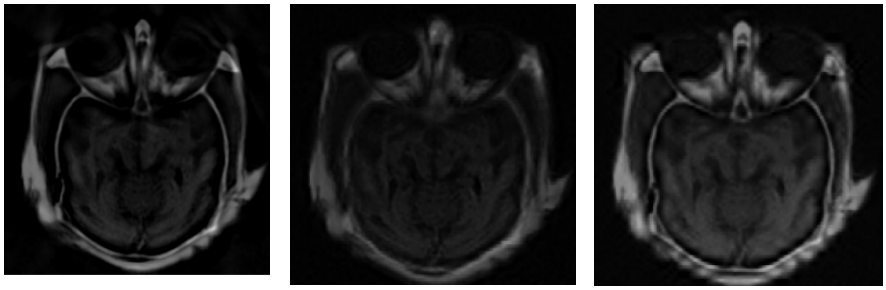

(a) Qu's method

(b) Richa's method

(c) Sudeb's method

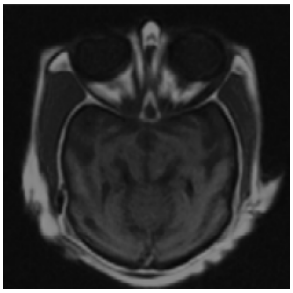

(d) Liu's method

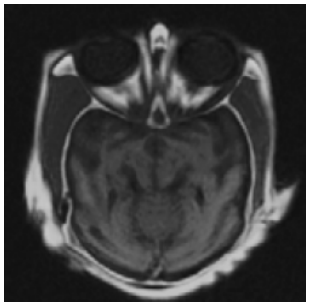

(e) Proposed method

Figure 3. The fusion results of Figure 2(a) and (b).

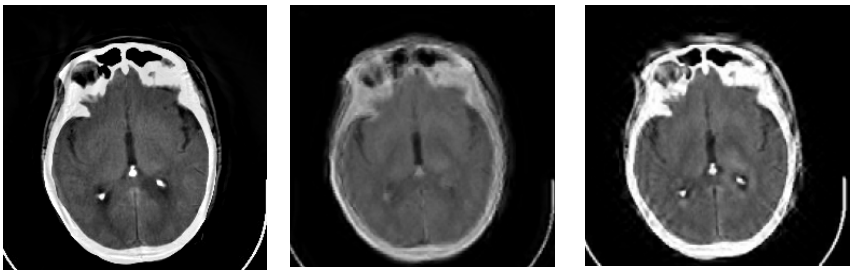

(a) Qu's method (b) Richa's method (c) Sudeb's method

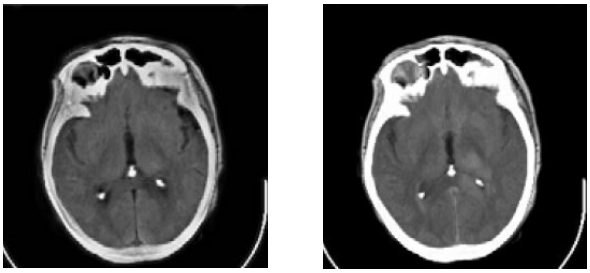

(d) Liu's method (e) Proposed method

Figure 4. The fusion results Figure 2(c) and (d).

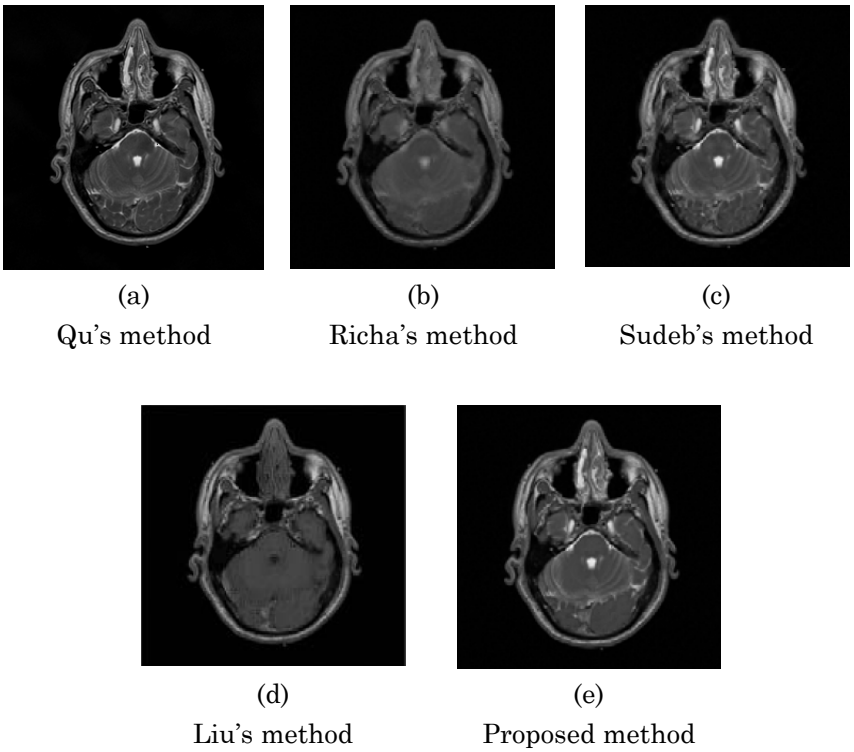

(a) Qu's method (b) Richa's method (c) Sudeb's method

(d) Liu's method (e) Proposed method

Figure 5. The fusion results Figure 2(e) and (f).

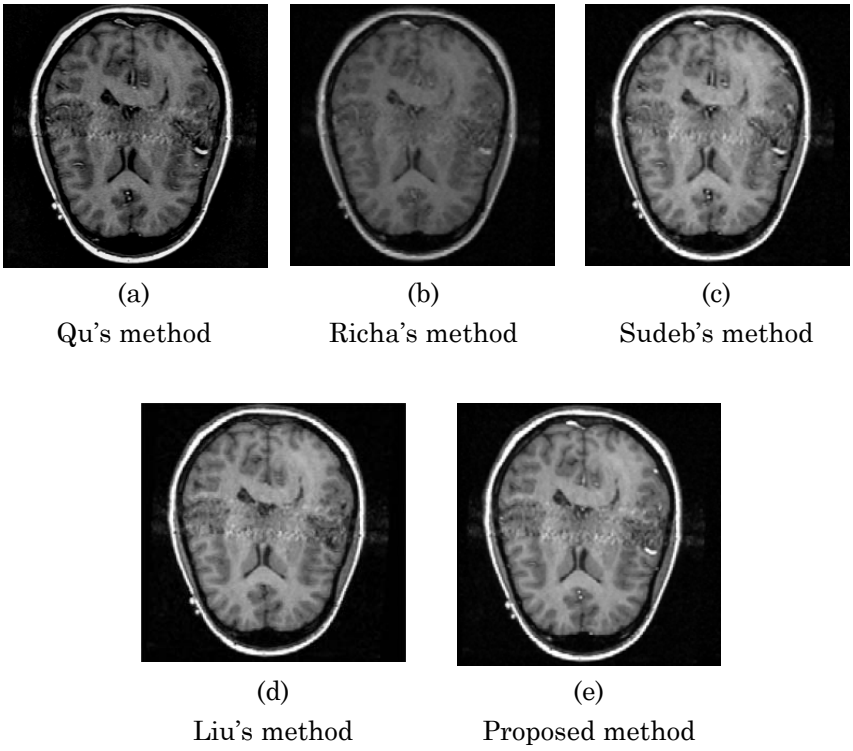

Figure 6. The fusion results Figure 2(g) and (h).

The Qu's algorithm gives baseline MI and $Q^{AB/F}$ value according to the objective evaluation shown in Table 1. The Richa's method gives baseline visual results shown in Figure 3(b), Figure 4(b), Figure 5(b), and Figure 6(b). The fusion method based on proposed by Sudeb is better than Qu's method and Richa's method. However, the fused image in Figure 3(c) and Figure 6(c) by the Sudeb's method shows low contrast than by proposed method. Specially, the Figure 4(c) lacks of the ability that extracts image feature result in the degradation of fusion performance. Figure 5(d) by Liu's method lost necessary information with white colour in the middle of Figure 2(f). The proposed image theme can fused the most of useful information from the source images because the QWT's shift-invariance and the effective fusion rules. The results presented in

this example can demonstrate that our approach can fuse the medical image while retaining much more information than that of the other three methods.

Table 1. Performance evaluation of different method

Source Images	Metric	Qu's method	Richa's method	Sudeb's method	Liu's method	Proposed method
Group a	MI	1.6098	2.4211	2.7964	5.2703	**5.3644**
	$Q^{AB/F}$	0.5799	0.3917	0.3970	0.6454	**0.7937**
Group b	MI	2.9896	3.1541	3.2194	3.6897	**3.8352**
	$Q^{AB/F}$	0.5457	0.2554	0.5189	0.5641	**0.5935**
Group c	MI	3.1538	3.6811	3.6111	4.0650	**4.7924**
	$Q^{AB/F}$	0.5373	0.3613	0.4909	0.5950	**0.6388**
Group d	MI	2.9984	3.4261	3.7506	**4.6924**	4.2615
	$Q^{AB/F}$	0.6667	0.5059	0.6173	0.6028	**0.7073**

6. Conclusion

In this paper, we have presented a new quaternion wavelet based multi-sensor medical image fusion method. The experimental results demonstrated that the proposed method outperforms the standard fusion methods in the fusion of different medical images. The proposed image fusion algorithm is an effective, efficient, and feasible algorithm. Finally, it is important to note that the proposed QWT-based fusion algorithm outperforms the RDWT-based, NSCT-based, and ripplet-based fusion algorithm in some cases.

References

[1] Zhiping Xu, Medical image fusion using multi-level local extrema, Information Fusion (2014), 38-48.

[2] Xuan Liu, Yue Zhou and Jiajun Wan, Image fusion based on shearlet transform and regional features, International Journal of Electronics and Communications 68(6) (2014), 471-477.

[3] R. Singh, M. Vatsa and A. Noore, Multimodal medical image fusion using redundant discrete wavelet transform, Advances in Pattern Recognition (2009), 232-235.

[4] L. Yang, B. L. Guo and W. Ni, Multimodality medical image fusion based on multiscale geometric analysis of contourlet transform, Neurocomputing 72(1) (2008), 203-211.

[5] Shuaiqi Liu, Jie Zhao, Peng Geng, Xiuling Liu and Yuchao Sun, Medical image fusion based on nonsubsampled direction complex wavelet transform, International Journal of Applied Mathematics and Machine Learning 1(1) (2014), 21-34.

[6] Das Sudeb and Kundu Malay Kumar, Ripplet based multimodality medical image fusion using pulse-coupled neural network and modified spatial frequency, International Conference on Recent Trends in Information Systems (2011), 229-234.

[7] Liyong Ma and Naizhang Feng, Nonsubsampled contourlet transform based image fusion for ultrasound tomography, Journal of Nanoelectronics and Optoelectronics 7(2) (2012), 216-219.

[8] L. Wang, B. Li and L. F. Tian, A novel multi-modal medical image fusion method based on shift-invariant shearlet transform, Imaging Science Journal 61(7) (2013), 529-540.

[9] Oliver Rockinger, Image sequence fusion using a shift-invariant wavelet transform, IEEE International Conference on Image Processing 3 (1997), 288-291.

[10] Shuaiqi Liu, Shaohai Hu and Yang Xiao, Image separation using wavelet-complex shearlet dictionary, Journal of Systems Engineering and Electronics 25(2) (2014), 314-321.

[11] W. L. Chan, H. Choi and R. G. Baraniuk, Coherent multiscale image processing using dual-tree quaternion wavelets, IEEE Transaction on Image Process 17(2) (2008), 1069-1082.

[12] Bayro-Corrochano Eduardo, The theory and use of the quaternion wavelet transform, Journal of Mathematical Imaging and Vision 24(1) (2006), 19-35.

[13] Yipeng Liu, Jing Jin, Qiang Wang, Yi Shen and Xiaoqiu Dong, Region level based multi-focus image fusion using quaternion wavelet and normalized cut, Signal Processing 97 (2014), 9-30.

[14] Jun Zhou, Yi Xu and Xiaokang Yang, Quaternion wavelet phase based stereo matching for uncalibrated images, Pattern Recognition Letters 28(12) (2007), 1509-1522.

[15] J. W. Huang, Q. S. Yun and X. H. Dai, A segmentation-based image coding algorithm using the features of human vision system, Journal of Image and Graphics 4(5) (1999), 400-404.

[16] Xiaobo Qu, Jingwen Yan, Hongzhi Xiao and Ziqian Zhu, Image fusion algorithm based on spatial frequency-motivated pulse coupled neural networks in nonsubsampled contourlet transform domain, Acta Automatica Sinica 34(12) (2008), 1508-1514.

[17] Umer Javed, Muhammad Mohsin Riaz, Abdul Ghafoor, Syed Sohaib Ali and Tanveer Ahmed Cheema, MRI and PET image fusion using fuzzy logic and image local features, The Scientific World Journal 2014: 708075.

http://dx.doi.org/10.1155/2014/708075

■